

**SO<sub>2</sub> noontime peak phenomenon in the North China Plain**

W. Y. Xu et al.

**SO<sub>2</sub> noontime peak phenomenon in the North China Plain**

W. Y. Xu<sup>1</sup>, C. S. Zhao<sup>1</sup>, L. Ran<sup>2</sup>, W. L. Lin<sup>3,4</sup>, P. Yan<sup>3,4</sup>, and X. B. Xu<sup>3</sup>

<sup>1</sup>Department of Atmospheric and Oceanic Sciences, School of Physics, Peking University, Beijing, China

<sup>2</sup>Key Laboratory of Middle Atmosphere and Global Environment Observation, Institute of Atmospheric Physics, Chinese Academy of Sciences, Beijing, China

<sup>3</sup>Key Laboratory for Atmospheric Chemistry, Institute of Atmospheric Composition, Chinese Academy of Meteorological Sciences, Beijing, China

<sup>4</sup>Meteorological Observation Center, China Meteorological Administration, Beijing, China

Received: 25 December 2013 – Accepted: 25 February 2014 – Published: 4 March 2014

Correspondence to: C. S. Zhao (zcs@pku.edu.cn)

Published by Copernicus Publications on behalf of the European Geosciences Union.

Title Page

Abstract

Introduction

Conclusions

References

Tables

Figures

◀

▶

◀

▶

Back

Close

Full Screen / Esc

Printer-friendly Version

Interactive Discussion



## Abstract

Frequent SO<sub>2</sub> noontime peak phenomenon was discovered in a detailed analysis on the SO<sub>2</sub> concentrations in the North China Plain (NCP). The possible causes and their contributions are analysed. The impacts of such a phenomenon on the sulphur cycle were studied and the implications of the phenomenon for atmospheric chemistry, cloud physics and climate were discussed. Different from the common SO<sub>2</sub> diurnal patterns with high nighttime concentrations, NCP witnessed high frequencies of SO<sub>2</sub> noontime peaks, with an occurrence frequency of 50–72 % at the four stations. Down-mixing of elevated pollution layers, plume transport processes, mountain-valley-winds and fog/high RH haze events were the possible causes. The contribution of each process varies from each other and from station to station, however, neither of those four processes can be neglected. SO<sub>2</sub> peaks occurring during noontime instead of nighttime will lead to a 13–35 % increase in sulphur dry deposition, 9–23 % increase in gas phase oxidation and 8–33 % increase in aqueous phase conversions, which will increase the hygroscopicity and the light scattering of aerosols, thus having important impacts on atmospheric chemistry, cloud physics and climate.

## 1 Introduction

High emissions and concentrations of sulphur dioxide (SO<sub>2</sub>) have been observed in the North China Plain (NCP) (Lin et al., 2012; Xu et al., 2011b; Zhao et al., 2013), which exerts great impacts on aerosol hygroscopicity and cloud physics (Liu et al., 2011). Yet, the special topography, emission distribution and meteorological conditions in the NCP have complicated the variation of SO<sub>2</sub> concentrations.

The diurnal variation of primary gas pollutants in polluted regions are typically characterized by morning and evening peaks, due to both the diurnal variations of the planetary boundary layer height (PBLH), emissions and the diurnal variation in photochemistry (Jacobson, 2002). The SO<sub>2</sub> diurnal variation pattern observed in both the

ACPD

14, 5653–5685, 2014

## SO<sub>2</sub> noontime peak phenomenon in the North China Plain

W. Y. Xu et al.

Title Page

Abstract

Introduction

Conclusions

References

Tables

Figures

◀

▶

◀

▶

Back

Close

Full Screen / Esc

Printer-friendly Version

Interactive Discussion



Yangtze-River-Delta region (Wang et al., 2002; Qi et al., 2012) and the Pearl-River-Delta region (Wang et al., 2001), as well as that observed in other parts of the world (Khemani et al., 1987; Psiloglou et al., 2013) seem to mostly comply to this rule, with a few exceptions found by Qi et al. (2012).

5 The chemical transformation of SO<sub>2</sub> is most rapid during noontime, when the photochemistry is most active and concentrations of oxidants such as the OH radical, H<sub>2</sub>O<sub>2</sub> and O<sub>3</sub> are highest (Hua et al., 2008; Ran et al., 2011). OH is the main oxidant for gas phase SO<sub>2</sub> scavenging, while H<sub>2</sub>O<sub>2</sub> and O<sub>3</sub> are the major oxidants in aqueous phase SO<sub>2</sub> scavenging processes (Seinfeld and Pandis, 2006). If SO<sub>2</sub> peak values occurred  
10 during noontime instead of during nighttime, sulphur conversions would be enhanced, increasing sulphate concentration in aerosols, leading to higher aerosol hygroscopicity and more light scattering.

Adame et al. (2012) reported rare cases of SO<sub>2</sub> peaking during noontime in Central-Southern Spain, which they attributed to transport from industrial regions. Antony Chen et al. (2001) observed a SO<sub>2</sub> noontime peak only in one out of five measurement periods in Maryland (USA), which were attributed to down-mixing from elevated sources. While this phenomenon seems to be a rare case all over world, several sites in the NCP shows averaged diurnal variation patterns with such variation characteristics (Lin et al., 2011, 2009, 2012, 2008). However, averaged diurnal patterns usually have large  
20 standard deviations due to the high seasonal variability of SO<sub>2</sub> and can be significantly influenced by strong pollution episodes. Thus the representativeness of such averaged profiles is unsure and how common such events were, what might have caused them or what the possible impacts such diurnal variation patterns might have is still not clear.

25 In this study, an elaborate investigation into the SO<sub>2</sub> diurnal variation pattern is made based on observations from four stations in the NCP. Possible causes for the noontime peaks and their relative importance are discussed. Finally, the possible impact of such events on the sulphur cycle is investigated and its influence on atmospheric chemistry and climate are pointed out.

## SO<sub>2</sub> noontime peak phenomenon in the North China Plain

W. Y. Xu et al.

Title Page

Abstract

Introduction

Conclusions

References

Tables

Figures

◀

▶

◀

▶

Back

Close

Full Screen / Esc

Printer-friendly Version

Interactive Discussion



## 2 Data and methodology

### 2.1 Site and measurements

Measurements of SO<sub>2</sub> and CO (Carbon Monoxide) were carried out at Wuqing meteorological station (WQ, 39.38° N 117.2° E, 7.4 m.a.s.l.) in the NCP during the Haze in China (HaChi) campaign (July 2009–January 2010). WQ is located in the heart of the plain region and has been proven to be highly representative of the polluted background (Xu et al., 2011).

Measurements from January 2009 to January 2010 at the Shangdianzi site (SDZ, 40.65° N, 117.12° E, 293.9 m.a.s.l.), the China Meteorological Administration site (CMA, 39.95° N, 116.32° E, 96 m.a.s.l.) and the Gucheng site (GCH, 39.13° N, 115.12° E, 15.1 m.a.s.l.) made by the Chinese Academy of Meteorological Sciences (Lin et al., 2011, 2009, 2012, 2008) were used as references.

Radiosonde data from March 2009 to February 2010 measured at the Nanjiao meteorological station (NJ, 39.8° N, 116.46° E, 33 m.a.s.l.) were used to analyse the temperature inversion within the PBLH to better understand the vertical mixing process. The radiosonde measurements were carried out every day at 8 a.m. The temperature inversion depth of each day was determined and the occurrence frequencies of different inversion depths were counted for spring (March–May 2009), summer (June–August 2009), autumn (September–November 2009) and winter (December 2009–February 2010), respectively.

The locations of the sites as well as the distribution of SO<sub>2</sub> column concentrations retrieved from the Ozone Monitoring Instrument (OMI) on board AURA satellite (OMSO2Readme file, [http://so2.gsfc.nasa.gov/Documentation/OMSO2ReleaseDetails\\_v111\\_0303.htm](http://so2.gsfc.nasa.gov/Documentation/OMSO2ReleaseDetails_v111_0303.htm)) are shown in Fig. 1.

The SO<sub>2</sub> polluted NCP is surrounded in the north by the Yan Mountains and to the west by the Taihang Mountains. The SDZ, CMA and GCH sites are aligned along a northeast – southwest line east to the Taihang Mountains, while WQ is about 80 km to the southeast of the CMA site. The SDZ, CMA, GCH and WQ sites respectively

## SO<sub>2</sub> noontime peak phenomenon in the North China Plain

W. Y. Xu et al.

Title Page

Abstract

Introduction

Conclusions

References

Tables

Figures

◀

▶

◀

▶

Back

Close

Full Screen / Esc

Printer-friendly Version

Interactive Discussion



represent the relatively clean background, the polluted urban, rural and suburban area. SO<sub>2</sub> concentrations are high in the south and relatively lower in the north.

A set of commercial trace gas instruments (Thermo Environmental Instruments Inc., USA C-series) has been used to continuously monitor various trace gases. SO<sub>2</sub> was measured with pulsed UV fluorescence analysers (TE 43CTL) and CO with gas filter correlation analysers (TE 48C). Measured gas concentrations were recorded as 1 min average mixing ratios by volume (ppbv), then averaged into 1 h resolutions. Details on the measurements and data calibration can be found in Lin et al. (2012) and Xu et al. (2011b).

## 2.2 Determination of SO<sub>2</sub> noon peak phenomenon

Due to the increased emissions, lower boundary layer heights and slower chemical conversions in winter, SO<sub>2</sub> concentrations show significant seasonal variations. In the study of the average SO<sub>2</sub> diurnal pattern, the enhanced signals of wintertime SO<sub>2</sub> data need to be avoided. SO<sub>2</sub> and CO concentrations were divided by the daily maximum value of each day, to acquire the daily normalized diurnal pattern.

Afterwards, patterns with peaks only occurring before 9 a.m. or after 4 p.m. were grouped into the Nighttime-Peak group (group 1), while patterns of peaks only occurring during 9 a.m. to 4 p.m. were classified into the Noontime-Peak group (group 2). Diurnal patterns with both a noontime and a nighttime peak during the same day were put into the Nighttime & Noontime group (group 3). The normalized diurnal variation patterns in each group were averaged and the standard error of the mean ( $sem = \sigma / \sqrt{n}$ ) was calculated for each hour of day. The occurrence frequency of each group was calculated for each month of 2009 and for the whole measurement period.

## 2.3 Four possible causes for the SO<sub>2</sub> noon peak phenomenon

Four possible causes for the SO<sub>2</sub> noontime peak phenomenon should be evaluated, the down-mixing for elevated SO<sub>2</sub> pollution layers, the transport of plumes, the influence of

## SO<sub>2</sub> noontime peak phenomenon in the North China Plain

W. Y. Xu et al.

Title Page

Abstract

Introduction

Conclusions

References

Tables

Figures



Back

Close

Full Screen / Esc

Printer-friendly Version

Interactive Discussion



**SO<sub>2</sub> noontime peak phenomenon in the North China Plain**

W. Y. Xu et al.

Title Page

Abstract

Introduction

Conclusions

References

Tables

Figures

◀

▶

◀

▶

Back

Close

Full Screen / Esc

Printer-friendly Version

Interactive Discussion



mountain-valley breezes and the impact of severe haze or fog events. The diurnal SO<sub>2</sub> profiles of group 2 and group 3 were analysed together with the according CO, wind, RH and temperature diurnal profiles to determine which of the above four causes has led to the occurrence of the noon peak. Then the contribution of each cause is yielded by dividing the number of noon peak cases caused by a certain factor with the total number of noon peak cases.

If the noon peak was caused by the down-mixing of elevated SO<sub>2</sub> pollution layers, the peak should occur during the early noon time (09:00–12:00 LT) when the PBL is developing. Thus, cases with SO<sub>2</sub> peaks occurring after the morning peak of CO along with the development of the PBL were filed under the down-mixing case category. The development of the PBL is represented by the increase in surface temperature.

CO has a relatively longer lifetime, thus is a very good tracer for pollution plumes. Days with the correlation coefficient between noontime SO<sub>2</sub> and CO reaching a significance level of 95 % were categorized into the plume transport case. Averaged correlation coefficients respectively reached 0.81, 0.82, 0.84 and 0.73 in SDZ, CMA, GCH and WQ.

Due to the topography of the NCP, all four sites are under the influence of mountain valley circulations, especially the SDZ, CMA and GCH sites. Winds often change from northern winds to southern ones during noontime (Lin et al., 2009, 2012). SO<sub>2</sub> noontime peak cases with the above described change in wind direction and with maximum wind speeds below 7 ms<sup>-1</sup> were counted into the mountain valley breezes case (Chen, 2009).

Severe haze or fog events are characterized by high RH values. For SDZ, GCH and WQ, the fog or severe haze event is defined as a case with RH exceeding 90 % for over 5 consecutive hours. Since CMA is located in urban Beijing and the site is surrounded by heat sources, RH measured at CMA seldom reaches 90 %. If the RHs at CMA exceed 80 % for over 5 consecutive hours and the other 3 stations simultaneously show RH greater than 90 %, then it is believed that CMA is also experiencing a fog or severe haze event.

## 2.4 Evaluation of the impacts of the SO<sub>2</sub> noon peak phenomenon on the sulphur cycle

To analyse how the SO<sub>2</sub> diurnal variation pattern influences upon the sulphur cycle, the WQ site of the HaChi Campaign has been selected to represent the polluted background of the NCP. Normalized SO<sub>2</sub> diurnal variation patterns, which were already grouped based on Sect. 2.2, were averaged respectively for summer (July–August), autumn (September–November) and winter (December–January). The occurrence frequency of each group in each season is calculated. The average SO<sub>2</sub> daily maximum value of each season, which is 20, 40 and 75 ppbv for summer, autumn and winter, respectively, is multiplied with the average normalized diurnal patterns to yield characteristic SO<sub>2</sub> diurnal concentration variation patterns for the three groups and for each season.

The characteristic SO<sub>2</sub> diurnal concentration variation patterns of the three groups will yield different dry deposition, gas phase oxidation and aqueous phase transformation amounts, which will be compared against each other. The occurrence frequency of the three groups will also be considered to show how the actual diurnal variation pattern influences the sulphur cycle.

### 2.4.1 The impact on dry deposition

The dry deposition velocity of SO<sub>2</sub> is under the influence of the surface type. Surfaces covered by vegetation usually show high SO<sub>2</sub> deposition rates during noontime and lower ones during nighttime due to transpiration processes (Tsai et al., 2010; Raymond et al., 2004). SO<sub>2</sub> concentration peaking during noontime instead of nighttime would increase SO<sub>2</sub> dry deposition fluxes, leading to increased acid depositions.

To study the impact of the SO<sub>2</sub> diurnal variation pattern on dry deposition fluxes, the diurnal variation of the dry deposition velocity  $v_d$  measured by Tsai et al. (2010) is used

## SO<sub>2</sub> noontime peak phenomenon in the North China Plain

W. Y. Xu et al.

Title Page

Abstract

Introduction

Conclusions

References

Tables

Figures

◀

▶

◀

▶

Back

Close

Full Screen / Esc

Printer-friendly Version

Interactive Discussion



and the dry deposition flux is calculated by:

$$F = C \cdot v_d, \quad (1)$$

where  $C$  is the  $\text{SO}_2$  concentration, which will be provided by the characteristic  $\text{SO}_2$  diurnal concentration variation pattern. The total daily dry deposition flux of group 2 and group 3 is compared against that of group 1. The daily dry deposition flux of the three groups are averaged weighted by the occurrence frequency of those three groups and is also compared against that of group 1. This will show how the  $\text{SO}_2$  diurnal variation characteristics in the NCP increase the dry depositions compared to the common nighttime peak pattern observed in other places of the world.

#### 2.4.2 The impact on gaseous oxidation

The NCAR Master Mechanism (NCAR-MM version 2.4) photochemical box model is used to calculate the homogeneous diurnal oxidation process of  $\text{SO}_2$  (Madronich, 2006; Madronich and Calvert, 1990). Detailed oxidation processes of  $\text{SO}_2$  with various atmospheric oxidants (e.g. OH,  $\text{O}_3$ ,  $\text{NO}_x$  and organic radicals) are included in the model. The concentration of  $\text{O}_3$  and  $\text{NO}_x$  are constrained according to the seasonally averaged diurnal profiles measured during the Hachi Summer Campaign, while that of VOCs could only be constrained according to summertime measurements (Ran et al., 2011).  $\text{SO}_2$  concentrations are constrained by the characteristic diurnal variation patterns of the three groups for the three seasons. The entrainment, dilution and dilution processes have been turned off to focus on the oxidation process.

The daily gas phase oxidized  $\text{SO}_2$  amount of group 2 and group 3 is compared against that of group 1. The daily gas phase oxidized  $\text{SO}_2$  amount of the three groups are averaged weighted by the occurrence frequency of those three groups and is also compared against that of group 1.

## $\text{SO}_2$ noontime peak phenomenon in the North China Plain

W. Y. Xu et al.

Title Page

Abstract

Introduction

Conclusions

References

Tables

Figures

⏪

⏩

◀

▶

Back

Close

Full Screen / Esc

Printer-friendly Version

Interactive Discussion



### 2.4.3 The impact on aqueous oxidation

The SO<sub>2</sub> aqueous oxidation process depends on the atmospheric liquid water content (LWC) as well as the concentration of atmospheric oxidants. For the aqueous phase oxidation of SO<sub>2</sub> the most important two oxidants are H<sub>2</sub>O<sub>2</sub> and O<sub>3</sub> (Seinfeld and Pandis, 2006).

The aqueous phase oxidized SO<sub>2</sub> amount can be estimated with the following two equations:

$$\Delta S(\text{IV}) = \left( k_1[\text{SO}_2 \cdot \text{H}_2\text{O}] + k_2[\text{HSO}_3^-] + k_3[\text{SO}_3^{2-}] \right) \cdot [\text{O}_3] \cdot \Delta t \cdot \text{LWC} \cdot 10^{-6}, \quad (2)$$

$$\Delta S(\text{IV}) = \frac{k_4[\text{H}^+][\text{HSO}_3^-]}{1 + k_5[\text{H}^+]} \cdot [\text{H}_2\text{O}_2] \cdot \Delta t \cdot \text{LWC} \cdot 10^{-6}, \quad (3)$$

where  $k_1, \dots, k_5$  are  $2.4 \times 10^4 \text{ mol}^{-1} \text{ s}^{-1}$ ,  $3.7 \times 10^5 \text{ mol}^{-1} \text{ s}^{-1}$ ,  $3.7 \times 10^5 \text{ mol}^{-1} \text{ s}^{-1}$ ,  $1.5 \times 10^9 \text{ mol}^{-1} \text{ s}^{-1}$ ,  $7.5 \times 10^7 \text{ mol}^{-2} \text{ s}^{-1}$ ,  $13 \text{ mol}^{-1}$ , respectively (Seinfeld and Pandis, 2006). The dissolved concentrations of SO<sub>2</sub>, O<sub>3</sub> and H<sub>2</sub>O<sub>2</sub> can be calculated with the Henry's Law.

Atmospheric LWC exists mostly in clouds, which makes the diurnal variation of atmospheric LWC very complicated. For this study, LWC is assumed to be a constant value  $0.029 \text{ g m}^{-3}$  throughout the day based on the aircraft measurements of clouds over the NCP (Deng et al., 2009). The pH value is fixed to 5.5 (Sun et al., 2010). The diurnal variation O<sub>3</sub> concentration pattern is set according to Sect. 2.4.2. The H<sub>2</sub>O<sub>2</sub> diurnal variation pattern shape is adopted from Hua et al. (2008), due to their relatively long measurement period. The daily maximum H<sub>2</sub>O<sub>2</sub> value during summer is set according to measurements in Beijing (He et al., 2010), while those in autumn and winter are set to 0.9 and 0.3 based on the H<sub>2</sub>O<sub>2</sub> concentration ratio of autumn/winter to summer in (Sakugawa et al., 1990). The SO<sub>2</sub> concentration pattern is set according to the characteristic diurnal variation patterns of the three groups for the three seasons.

Title Page

Abstract

Introduction

Conclusions

References

Tables

Figures

◀

▶

◀

▶

Back

Close

Full Screen / Esc

Printer-friendly Version

Interactive Discussion



The daily aqueous phase oxidized SO<sub>2</sub> amount of group 2 and group 3 is compared against that of group 1. The occurrence frequency weighting averaged results of the three groups is also compared against that of group 1.

It should be noted that, certain uncertainties will be introduced into this estimation by assuming that trace gas concentrations at cloud level are the same as at ground level. However, the uncertainty will be only shown in the absolute aqueous oxidized amount and will not have influences on the inter-comparison between the groups.

### 3 Results and discussions

#### 3.1 SO<sub>2</sub> noontime peak phenomenon in the NCP

While the SO<sub>2</sub> diurnal variation in other parts of the world were typically characterized by higher values during the night and lower ones during the day, the NCP has revealed inversed SO<sub>2</sub> variation characteristics.

Figure 2a–d displays the season-diurnal variation of SO<sub>2</sub> concentrations at SDZ, CMA, GCH and WQ, respectively. It can be noted that SO<sub>2</sub> concentrations are usually higher in cold seasons, due to enhanced emissions, weakened removal processes and lower PBLH. Significantly elevated SO<sub>2</sub> values during noontime throughout all the seasons were found at the GCH and WQ stations (Fig. 2c and d). At SDZ, high SO<sub>2</sub> concentrations in all but the winter season occur during noontime (Fig. 2a). At CMA, noontime SO<sub>2</sub> peaks could only be observed in spring and autumn, while in winter high SO<sub>2</sub> concentrations occur both during early noon and nighttime (Fig. 2b).

The SO<sub>2</sub> noontime peak seems to be a common phenomenon throughout the NCP region, especially at the WQ and GCH site, at which the measurements are more representative of the regional background pollution. However, how frequent such events occur, what the causes are and what impacts they may have on atmospheric chemistry, cloud physics and climate is still unknown.

## SO<sub>2</sub> noontime peak phenomenon in the North China Plain

W. Y. Xu et al.

Title Page

Abstract

Introduction

Conclusions

References

Tables

Figures

◀

▶

◀

▶

Back

Close

Full Screen / Esc

Printer-friendly Version

Interactive Discussion



**SO<sub>2</sub> noontime peak phenomenon in the North China Plain**

W. Y. Xu et al.

Title Page

Abstract

Introduction

Conclusions

References

Tables

Figures

◀

▶

◀

▶

Back

Close

Full Screen / Esc

Printer-friendly Version

Interactive Discussion



For the study of the average diurnal pattern, normalized diurnal patterns were calculated and classified into the Nighttime-Peak group (group 1), the Noontime-Peak group (group 2) and the Nighttime & Noontime group (group 3). The average normalized diurnal variation pattern of each group, the according sem and the occurrence frequency of each group is displayed in Fig. 3.

As depicted in Fig. 3a1–d1, the total SO<sub>2</sub> noontime peak occurrence frequency (group 2 + group 3) respectively reached 58 %, 50 %, 72 % and 69 % at the SDZ, CMA, GCH and WQ station. Days with only one noontime peak were more common (SDZ: 43 %, CMA: 31 %, GCH: 47 %, WQ: 44 %), while cases with both noontime and nighttime peaks also often occurred (SDZ: 15 %, CMA: 19 %, GCH: 25 %, WQ: 25 %). At SDZ, GCH and WQ, the average normalized SO<sub>2</sub> concentration reaches its peak at 12 a.m., while at CMA the peak occurs between 10 to 11 a.m. The averaged diurnal variation pattern of group 3 show lower peak values than group 2 and the peaks tend to occur 1 h earlier than in group 2. However, both group 2 and group 3 for SO<sub>2</sub> reveal distinct noontime peaks.

The averaged diurnal patterns of CO for the CMA, GCH and WQ sites resemble each other in shape. The normalized CO concentrations of group 2 and group 3 all show peaks at 9 a.m., which can also be seen as late morning peaks. At SDZ, the CO peak of group 2 occurs between 12 a.m. to 2 p.m., while that of group 3 is also found between 9–10 a.m. The total noontime peak occurrence frequency of CO for SDZ, CMA, GCH and WQ is 30 %, 39 %, 40 % and 55 %, respectively.

The total occurrence frequencies of noontime SO<sub>2</sub> peaks in each month for the four stations are listed in Table 1. Distinctly higher occurrence frequencies during warmer seasons were found in SDZ, while in CMA the occurrence frequencies are high in spring and autumn. Noontime peak occurrence frequencies in GCH show less regular seasonal variations, while those in WQ are relatively lower in summer and higher in autumn and winter.

It can be concluded that, the SO<sub>2</sub> noontime peak phenomenon occurs frequently at the NCP sites, regardless of seasons. The average peak is mostly reached at 12 a.m.



in Fig. 5a1-a4. Down-mixing case samples take up 34 %, 30 %, 43 % and 52 % of the noontime peaks at SDZ, CMA, GCH and WQ, respectively (Table 2a).

The transport of SO<sub>2</sub> plumes can result in sudden increases of local SO<sub>2</sub> concentrations. The plume transport process is characterized by the cohesive variation of SO<sub>2</sub> and CO. The average normalized SO<sub>2</sub>, CO and temperature profiles in the plume transport case can be seen in Fig. 5b1–b4. Although SO<sub>2</sub> shows a peak between 9 and 12 a.m., the occurrence time of the peaks caused by plume transport processes was rather random. This process respectively explains 21 %, 46 %, 20 % and 30 % of the noontime peaks at SDZ, CMA, GCH and WQ (Table 2b). It should be noted that, due to our classification method, cases with SO<sub>2</sub> and CO both having a late morning peak are also included into this category.

Mountain valley circulations lead to diurnal variations in wind directions, thus resulting in a diurnal variation in pollutant transport. Due to the topography of the NCP, all four sites are under the influence of mountain valley circulations, especially the SDZ, CMA and GCH sites. Winds often change from northern winds to southern ones during noontime. Due to the stronger SO<sub>2</sub> emissions and resulting higher concentrations in the southern part of the NCP (Fig. 1), southern winds will aid the transport of polluted air masses to our stations. The average diurnal patterns in the mountain valley breezes case are shown in Fig. 5a3–d3. A change in wind direction takes place between 8 a.m. to 12 a.m., while SO<sub>2</sub> starts increasing before noon and reaches its peak between 12 a.m. and 4 p.m. at all four stations. As can be seen in Table 2c, the mountain valley breeze factor can respectively explain 40 %, 20 %, 20 % and 6 % of the noontime peaks occurring in SDZ, CMA, GCH and WQ. Since SDZ is a relatively clean background site, the mountain-valley breeze will not only cause increasing noontime SO<sub>2</sub> concentrations but also increasing CO concentrations. This explains why only the SDZ site showed noontime CO peaks in Fig. 3.

Aerosol and fog liquid water can serve as an efficient sink for SO<sub>2</sub>. SO<sub>2</sub> is a soluble gas, which can be scavenged effectively through aqueous phase reactions in fog or wet aerosol particles (Pandis et al., 1992). Fog and high RH haze events usually occur

## SO<sub>2</sub> noontime peak phenomenon in the North China Plain

W. Y. Xu et al.

Title Page

Abstract

Introduction

Conclusions

References

Tables

Figures

◀

▶

◀

▶

Back

Close

Full Screen / Esc

Printer-friendly Version

Interactive Discussion



## SO<sub>2</sub> noontime peak phenomenon in the North China Plain

W. Y. Xu et al.

Title Page

Abstract

Introduction

Conclusions

References

Tables

Figures

◀

▶

◀

▶

Back

Close

Full Screen / Esc

Printer-friendly Version

Interactive Discussion



during nighttime and persist until the temperature rises up in the morning, leading to low nighttime SO<sub>2</sub> concentrations. Additionally, such events are typically characterized by surface temperature inversions, which will prevent the down-mixing of elevated SO<sub>2</sub> emissions (Jacobson, 2002). With the increasing temperature in the morning, the RH will decrease, weakening the SO<sub>2</sub> scavenging process. The temperature inversion will vanish, allowing for the down-mixing of SO<sub>2</sub> from aloft. Averaged normalized SO<sub>2</sub>, CO and RH profiles in the fog or severe haze case are shown in Fig. 5d1–d4. SO<sub>2</sub> peaks were reached typically between 12 a.m. and 16 p.m., depending on how long the fog or high RH event lasted. Such events caused 5%, 4%, 18% and 12% of the noontime peak events at SDZ, CMA, GCH and WQ, respectively.

### 3.3 Impacts of SO<sub>2</sub> noontime peak phenomenon on the sulphur cycle

SO<sub>2</sub> peaks occurring during noontime instead of nighttime might have remarkable impacts on human health, environment and climate. Higher SO<sub>2</sub> concentrations during daytime will not only pose higher health risks for humans, but also change the sulphur cycle.

For surfaces covered with vegetation, dry deposition processes are typically most dynamic during noontime due to transpiration processes (Tsai et al., 2010; Raymond et al., 2004), thus noontime SO<sub>2</sub> peaks may create more acid deposition than common nighttime peak variation patterns. The calculated diurnal dry deposition fluxes based on the diurnal dry deposition velocity in Tsai et al. (2010) and the characteristic SO<sub>2</sub> diurnal variations of the three groups in WQ during autumn are shown in Fig. 6. Group 2 and 3 show significantly higher dry deposition fluxes than group1 during 8 a.m. to 6 p.m. (LT), while for the other time periods the dry deposition fluxes of the three groups are similar to one another. The estimated daily deposition fluxes for summer, winter and autumn in WQ are listed in Table 3. Seasonally, dry deposition fluxes are higher during colder seasons than during warmer ones, due to elevated SO<sub>2</sub> concentrations and due to the fact that seasonal variations in dry deposition rates were not considered. Within the same season, the occurrence time of the SO<sub>2</sub> peak had major impacts on the

5 daily dry deposition fluxes. The results of group 2 show a 22–46% increase in daily dry deposition flux compared to those of group 1, while those of group 3 show a 44–62% increase. Considering the occurrence frequency of the three diurnal patterns, the weighting averaged daily dry deposition fluxes show increases of 13–35% relative to the common nighttime peak case, with the lowest increase occurring during summer and the highest one during autumn.

10 Atmospheric photochemistry is most active during noontime due to favourable radiative conditions. The simulated SO<sub>2</sub> gas phase conversion processes for the three SO<sub>2</sub> diurnal variation patterns in WQ during autumn are displayed in Fig. 7. Due to the fact that deposition processes have been turned off in the simulations, S(VI) products will accumulate in the air parcel. Accumulated S(VI) concentrations of group 3 are the highest throughout the day, while that of group 2 exceeds that of group 1 after 10 a.m. The SO<sub>2</sub> oxidation rates of group 2 and 3 during noontime are significantly higher than those of group 1. The simulated daily gas phase SO<sub>2</sub> conversion amount for summer, winter and autumn in WQ are listed in Table 4. Despite the weakened photochemistry during winter, the high SO<sub>2</sub> concentration in winter has led to higher gas phase oxidized SO<sub>2</sub> amounts. SO<sub>2</sub> noontime peak patterns could also increase the daily gas phase oxidized SO<sub>2</sub> amount. The results of group 2 show a 15–28% increase in gas phase oxidized amount compared to those of group 1, while those of group 3 show a 28–43% increase. Considering the occurrence frequency of the three diurnal patterns, the weighting averaged gas phase oxidized amounts show increases of 9–23% relative to the common nighttime peak case, with the lowest increase occurring during summer and the highest one in winter.

25 Concentrations of atmospheric oxidants that are important in SO<sub>2</sub> aqueous phase reactions also reach their peaks during noontime. Assuming a constant LWC throughout the day and assuming that concentrations near clouds are similar to the surface concentrations, the estimated SO<sub>2</sub> aqueous phase conversion rate for the three SO<sub>2</sub> diurnal variation patterns in WQ during autumn are displayed Fig. 8. SO<sub>2</sub> conversion amounts of group 2 and 3 are significantly higher than those of group 1 during 8 a.m.

## SO<sub>2</sub> noontime peak phenomenon in the North China Plain

W. Y. Xu et al.

Title Page

Abstract

Introduction

Conclusions

References

Tables

Figures

◀

▶

◀

▶

Back

Close

Full Screen / Esc

Printer-friendly Version

Interactive Discussion





## SO<sub>2</sub> noontime peak phenomenon in the North China Plain

W. Y. Xu et al.

Title Page

Abstract

Introduction

Conclusions

References

Tables

Figures

◀

▶

◀

▶

Back

Close

Full Screen / Esc

Printer-friendly Version

Interactive Discussion

noontime peak phenomenon significantly speeds up the sulphur cycle. Compared to the nighttime SO<sub>2</sub> peak case, which was observed all around the world, WQ respectively experienced 13–35 %, 9–23 % and 8–33 % enhancement in sulphur dry depositions, gas phase oxidations and aqueous phase conversions due to the frequently occurring SO<sub>2</sub> noontime peak phenomenon.

SO<sub>2</sub> peaks occurring during noontime instead of nighttime has led to more acidic deposition. Aerosols in the NCP will show higher sulphate fractions and become more hygroscopic. This will promote the light scattering effect of aerosols and thus may have important impacts on regional climate. Higher SO<sub>2</sub> concentrations during daytime will also pose higher health risks for human. The potential impacts of such a phenomenon on human health, environment and climate should be studied in detail in the future.

*Acknowledgements.* This work is supported by the National 973 project of China (2011CB403402), National Natural Science Foundation of China (41375134), Beijing Natural Science Foundation (8131003) and the Basic Research Fund of Chinese Academy of Meteorological Sciences (2011Z003).

## References

- Adame, J. A., Notario, A., Villanueva, F., and Albaladejo, J.: Application of cluster analysis to surface ozone, NO<sub>2</sub> and SO<sub>2</sub> daily patterns in an industrial area in central-southern Spain measured with a DOAS system, *Sci. Total Environ.*, 429, 281–291, doi:10.1016/j.scitotenv.2012.04.032, 2012.
- Antony Chen, L. W., Doddridge, B. G., Dickerson, R. R., Chow, J. C., Mueller, P. K., Quinn, J., and Butler, W. A.: Seasonal variations in elemental carbon aerosol, carbon monoxide and sulfur dioxide: implications for sources, *Geophys. Res. Lett.*, 28, 1711–1714, doi:10.1029/2000GL012354, 2001.
- Chen, Y.: The impact of local circulation on the distribution and transport of atmospheric pollutants in Beijing, M.S. thesis, Department of Atmospheric and Oceanic Sciences, Peking University, Beijing, 2009.

## SO<sub>2</sub> noontime peak phenomenon in the North China Plain

W. Y. Xu et al.

Title Page

Abstract

Introduction

Conclusions

References

Tables

Figures

◀

▶

◀

▶

Back

Close

Full Screen / Esc

Printer-friendly Version

Interactive Discussion



- Chen, Y., Zhao, C., Zhang, Q., Deng, Z., Huang, M., and Ma, X.: Aircraft study of Mountain Chimney Effect of Beijing, China, *J. Geophys. Res.-Atmos.*, 114, D08306, doi:10.1029/2008JD010610, 2009.
- Deng, Z., Zhao, C., Zhang, Q., Huang, M., and Ma, X.: Statistical analysis of microphysical properties and the parameterization of effective radius of warm clouds in Beijing area, *Atmos. Res.*, 93, 888–896, doi:10.1016/j.atmosres.2009.04.011, 2009.
- He, S. Z., Chen, Z. M., Zhang, X., Zhao, Y., Huang, D. M., Zhao, J. N., Zhu, T., Hu, M., and Zeng, L. M.: Measurement of atmospheric hydrogen peroxide and organic peroxides in Beijing before and during the 2008 Olympic Games: chemical and physical factors influencing their concentrations, *J. Geophys. Res.-Atmos.*, 115, D17307, doi:10.1029/2009JD013544, 2010.
- Hua, W., Chen, Z. M., Jie, C. Y., Kondo, Y., Hofzumahaus, A., Takegawa, N., Chang, C. C., Lu, K. D., Miyazaki, Y., Kita, K., Wang, H. L., Zhang, Y. H., and Hu, M.: Atmospheric hydrogen peroxide and organic hydroperoxides during PRIDE-PRD'06, China: their concentration, formation mechanism and contribution to secondary aerosols, *Atmos. Chem. Phys.*, 8, 6755–6773, doi:10.5194/acp-8-6755-2008, 2008.
- Jacobson, M. Z.: *Atmospheric Pollution: History, Science, and Regulation*, Cambridge University Press, Cambridge, 2002.
- Khemani, L. T., Momin, G. A., and Singh, G.: Variations in trace gas concentrations in different environments in India, *Pageoph*, 125, 167–181, doi:10.1007/BF00878620, 1987.
- Lin, W., Xu, X., Zhang, X., and Tang, J.: Contributions of pollutants from North China Plain to surface ozone at the Shangdianzi GAW Station, *Atmos. Chem. Phys.*, 8, 5889–5898, doi:10.5194/acp-8-5889-2008, 2008.
- Lin, W., Xu, X., Ge, B., and Zhang, X.: Characteristics of gaseous pollutants at Gucheng, a rural site southwest of Beijing, *J. Geophys. Res.*, 114, D00G14, doi:10.1029/2008jd010339, 2009.
- Lin, W., Xu, X., Ge, B., and Liu, X.: Gaseous pollutants in Beijing urban area during the heating period 2007–2008: variability, sources, meteorological, and chemical impacts, *Atmos. Chem. Phys.*, 11, 8157–8170, doi:10.5194/acp-11-8157-2011, 2011.
- Lin, W., Xu, X., Ma, Z., Zhao, H., Liu, X., and Wang, Y.: Characteristics and recent trends of sulfur dioxide at urban, rural, and background sites in North China: effectiveness of control measures, *J. Environ. Sci.*, 24, 34–49, doi:10.1016/S1001-0742(11)60727-4, 2012.
- Liu, H. J., Zhao, C. S., Nekat, B., Ma, N., Wiedensohler, A., van Pinxteren, D., Spindler, G., Müller, K., and Herrmann, H.: Aerosol hygroscopicity derived from size-segregated chemical

**SO<sub>2</sub> noontime peak phenomenon in the North China Plain**

W. Y. Xu et al.

Title Page

Abstract

Introduction

Conclusions

References

Tables

Figures

◀

▶

◀

▶

Back

Close

Full Screen / Esc

Printer-friendly Version

Interactive Discussion



composition and its parameterization in the North China Plain, *Atmos. Chem. Phys. Discuss.*, 13, 20885–20922, doi:10.5194/acpd-13-20885-2013, 2013.

Liu, P. F., Zhao, C. S., Göbel, T., Hallbauer, E., Nowak, A., Ran, L., Xu, W. Y., Deng, Z. Z., Ma, N., Mildenerger, K., Henning, S., Stratmann, F., and Wiedensohler, A.: Hygroscopic properties of aerosol particles at high relative humidity and their diurnal variations in the North China Plain, *Atmos. Chem. Phys.*, 11, 3479–3494, doi:10.5194/acp-11-3479-2011, 2011.

Madronich, S.: Chemical evolution of gaseous air pollutants down-wind of tropical megacities: Mexico City case study, *Atmos. Environ.*, 40, 6012–6018, doi:10.1016/j.atmosenv.2005.08.047, 2006.

Madronich, S. and Calvert, J. G.: Permutation reactions of organic peroxy radicals in the troposphere, *J. Geophys. Res.-Atmos.*, 95, 5697–5715, doi:10.1029/JD095iD05p05697, 1990.

OMSO<sub>2</sub> Release Specific Information: available at: [http://so2.gsfc.nasa.gov/Documentation/OMSO2ReleaseDetails\\_v111\\_0303.htm](http://so2.gsfc.nasa.gov/Documentation/OMSO2ReleaseDetails_v111_0303.htm) (last access: 28 March 2013), 2013.

Pandis, S. N., Seinfeld, J. H., and Pilinis, C.: Heterogeneous sulfate production in an urban fog, *Atmos. Environ. A-Gen.*, 26, 2509–2522, doi:10.1016/0960-1686(92)90103-R, 1992.

Psiloglou, B., Larissi, I., Petrakis, M., Paliatsos, A., Antoniou, A., and Viras, L.: Case studies on summertime measurements of O<sub>3</sub>, NO<sub>2</sub>, and SO<sub>2</sub> with a DOAS system in an urban semi-industrial region in Athens, Greece, *Environ. Monit. Assess.*, 185, 7763–7774, doi:10.1007/s10661-013-3134-2, 2013.

Qi, H., Lin, W., Xu, X., Yu, X., and Ma, Q.: Significant downward trend of SO<sub>2</sub> observed from 2005 to 2010 at a background station in the Yangtze Delta region, China, *Sci. China Chem.*, 55, 1451–1458, doi:10.1007/s11426-012-4524-y, 2012.

Ran, L., Zhao, C. S., Xu, W. Y., Lu, X. Q., Han, M., Lin, W. L., Yan, P., Xu, X. B., Deng, Z. Z., Ma, N., Liu, P. F., Yu, J., Liang, W. D., and Chen, L. L.: VOC reactivity and its effect on ozone production during the HaChi summer campaign, *Atmos. Chem. Phys.*, 11, 4657–4667, doi:10.5194/acp-11-4657-2011, 2011.

Raymond, H. A., Yi, S.-M., Moumen, N., Han, Y., and Holsen, T. M.: Quantifying the dry deposition of reactive nitrogen and sulfur containing species in remote areas using a surrogate surface analysis approach, *Atmos. Environ.*, 38, 2687–2697, doi:10.1016/j.atmosenv.2004.02.011, 2004.

Sakugawa, H., Tsai, W., Kaplan, I. R., and Cohen, Y.: Factors controlling the photochemical generation of gaseous H<sub>2</sub>O<sub>2</sub> in the Los Angeles atmosphere, *Geophys. Res. Lett.*, 17, 93–96, doi:10.1029/GL017i001p00093, 1990.

**SO<sub>2</sub> noontime peak phenomenon in the North China Plain**

W. Y. Xu et al.

Title Page

Abstract

Introduction

Conclusions

References

Tables

Figures

◀

▶

◀

▶

Back

Close

Full Screen / Esc

Printer-friendly Version

Interactive Discussion



Sun, M., Wang, Y., Wang, T., Fan, S., Wang, W., Li, P., Guo, J., and Li, Y.: Cloud and the corresponding precipitation chemistry in south China: water-soluble components and pollution transport, *J. Geophys. Res.-Atmos.*, 115, D22303, doi:10.1029/2010JD014315, 2010.

Tsai, J.-L., Chen, C.-L., Tsuang, B.-J., Kuo, P.-H., Tseng, K.-H., Hsu, T.-F., Sheu, B.-H., Liu, C.-P., and Hsueh, M.-T.: Observation of SO<sub>2</sub> dry deposition velocity at a high elevation flux tower over an evergreen broadleaf forest in Central Taiwan, *Atmos. Environ.*, 44, 1011–1019, doi:10.1016/j.atmosenv.2009.12.022, 2010.

Wang, S., Hao, J., Ho, M. S., Li, J., and Lu, Y.: Intake fractions of industrial air pollutants in China: estimation and application, *Sci. Total Environ.*, 354, 127–141, doi:10.1016/j.scitotenv.2005.01.045, 2006.

Wang, T., Cheung, V. T. F., Lam, K. S., Kok, G. L., and Harris, J. M.: The characteristics of ozone and related compounds in the boundary layer of the South China coast: temporal and vertical variations during autumn season, *Atmos. Environ.*, 35, 2735–2746, doi:10.1016/s1352-2310(00)00411-8, 2001.

Wang, T., Cheung, T. F., Li, Y. S., Yu, X. M., and Blake, D. R.: Emission characteristics of CO, NO<sub>x</sub>, SO<sub>2</sub> and indications of biomass burning observed at a rural site in eastern China, *J. Geophys. Res.*, 107, 4157, doi:10.1029/2001jd000724, 2002.

Xu, W. Y., Zhao, C. S., Ran, L., Deng, Z. Z., Liu, P. F., Ma, N., Lin, W. L., Xu, X. B., Yan, P., He, X., Yu, J., Liang, W. D., and Chen, L. L.: Characteristics of pollutants and their correlation to meteorological conditions at a suburban site in the North China Plain, *Atmos. Chem. Phys.*, 11, 4353–4369, doi:10.5194/acp-11-4353-2011, 2011.

Yang, D., Wang, Z., and Zhang, R.: Estimating air quality impacts of elevated point source emissions in Chongqing, China, *Aerosol Air Qual. Res.*, 8, 279–294, doi:10.4209/aaqr.2008.02.0005, 2008.

Zhao, P. S., Dong, F., He, D., Zhao, X. J., Zhang, X. L., Zhang, W. Z., Yao, Q., and Liu, H. Y.: Characteristics of concentrations and chemical compositions for PM<sub>2.5</sub> in the region of Beijing, Tianjin, and Hebei, China, *Atmos. Chem. Phys.*, 13, 4631–4644, doi:10.5194/acp-13-4631-2013, 2013.

Zhou, Y., Levy, J. I., Hammitt, J. K., and Evans, J. S.: Estimating population exposure to power plant emissions using CALPUFF: a case study in Beijing, China, *Atmos. Environ.*, 37, 815–826, doi:10.1016/S1352-2310(02)00937-8, 2003.

## SO<sub>2</sub> noontime peak phenomenon in the North China Plain

W. Y. Xu et al.

Title Page

Abstract

Introduction

Conclusions

References

Tables

Figures

◀

▶

◀

▶

Back

Close

Full Screen / Esc

Printer-friendly Version

Interactive Discussion



**Table 1.** Seasonal variation of noontime peak occurrence frequency.

Month	Noontime Peak Occurrence Frequency (%)			
	SDZ	CMA	GCH	WQ
Jan	39	33	71	–
Feb	32	29	89	–
Mar	26	39	65	–
Apr	33	70	70	–
May	42	47	52	–
Jun	60	50	50	–
Jul	67	32	81	40
Aug	71	55	68	48
Sep	73	67	63	69
Oct	77	58	71	62
Nov	53	52	57	62
Dec	37	16	65	64

## SO<sub>2</sub> noontime peak phenomenon in the North China Plain

W. Y. Xu et al.

Title Page

Abstract

Introduction

Conclusions

References

Tables

Figures

◀

▶

◀

▶

Back

Close

Full Screen / Esc

Printer-friendly Version

Interactive Discussion



**Table 2.** SO<sub>2</sub> noontime peak occurrence frequency and the fraction of noontime peaks caused by **(a)** down-mixing due to PBL processes, **(b)** plume transport, **(c)** mountain valley breezes and **(d)** fog or severe haze events.

Station	SDZ	CMA	GCH	WQ
Total Sample Count	356	374	395	180
Noontime Peak Sample Count (Occurrence Frequency)	179 (50 %)	165 (44 %)	269 (68 %)	105 (58 %)
<b>(a)</b> Down-mixing caused Noontime Peak Sample Count	60 (34 %)	50 (30 %)	117 (43 %)	55 (52 %)
<b>(b)</b> Plume transport caused Noontime Peak Sample Count	38 (21 %)	76 (46 %)	53 (20 %)	31 (30 %)
<b>(c)</b> Mountain Valley Breeze caused Noontime Peak Sample Count	72 (40 %)	33 (20 %)	53 (20 %)	6 (6 %)
<b>(d)</b> Fog or severe haze events caused Noontime Peak Sample Count	9 (5 %)	6 (4 %)	49 (18 %)	13 (12 %)

## SO<sub>2</sub> noontime peak phenomenon in the North China Plain

W. Y. Xu et al.

Title Page

Abstract

Introduction

Conclusions

References

Tables

Figures

◀

▶

◀

▶

Back

Close

Full Screen / Esc

Printer-friendly Version

Interactive Discussion



**Table 3.** Estimated SO<sub>2</sub> dry deposition flux for the three different SO<sub>2</sub> diurnal variation patterns, the occurrence frequency (of the three groups) weighting averaged value and the relative increase compared to the nighttime peak case.

Case	SO <sub>2</sub> dry deposition flux (gm <sup>-2</sup> day <sup>-1</sup> )		
	[Increase relative to nighttime peak case (%)]		
	Summer	Autumn	Winter
Nighttime Peak	0.0065	0.014	0.028
Noontime Peak	0.0079 (22 %)	0.020 (46 %)	0.035 (27 %)
Nighttime + Noontime Peak	0.0093 (44 %)	0.022 (58 %)	0.045 (62 %)
Weighting average	0.0073 (13 %)	0.019 (35 %)	0.035 (28 %)

## SO<sub>2</sub> noontime peak phenomenon in the North China Plain

W. Y. Xu et al.

Title Page

Abstract

Introduction

Conclusions

References

Tables

Figures

◀

▶

◀

▶

Back

Close

Full Screen / Esc

Printer-friendly Version

Interactive Discussion



**Table 4.** Simulated SO<sub>2</sub> gaseous oxidation amount for the three different SO<sub>2</sub> diurnal variation patterns, the occurrence frequency (of the three groups) weighting averaged value and the relative increase compared to the nighttime peak case.

Case	SO <sub>2</sub> gaseous oxidized amount (ppbv day <sup>-1</sup> ) [Increase relative to nighttime peak case (%)]		
	Summer	Autumn	Winter
Nighttime Peak	2.3	4.5	5.1
Noontime Peak	2.6 (15%)	5.7 (26%)	6.5 (28%)
Nighttime + Noontime Peak	2.9 (28%)	6.2 (38%)	7.3 (43%)
Weighting Average	2.5 (9%)	5.5 (21%)	6.2 (23%)

## SO<sub>2</sub> noontime peak phenomenon in the North China Plain

W. Y. Xu et al.

Title Page

Abstract

Introduction

Conclusions

References

Tables

Figures

◀

▶

◀

▶

Back

Close

Full Screen / Esc

Printer-friendly Version

Interactive Discussion



**Table 5.** Estimated SO<sub>2</sub> aqueous oxidation amount for the three different SO<sub>2</sub> diurnal variation patterns, the occurrence frequency (of the three groups) weighting averaged value and the relative increase compared to the nighttime peak case.

Case	SO <sub>2</sub> aqueous oxidized amount (ppbv day <sup>-1</sup> ) [Increase relative to nighttime peak case (%)]		
	Summer	Autumn	Winter
Nighttime Peak	86.5	64.2	62.4
Noontime Peak	97.5 (13 %)	91.6 (43 %)	77.2 (24 %)
Nighttime + Noontime Peak	110.9 (28 %)	99.7 (55 %)	100.6 (61 %)
Weighting average	93.3 (8 %)	85.5 (33 %)	78.8 (26 %)

## SO<sub>2</sub> noontime peak phenomenon in the North China Plain

W. Y. Xu et al.

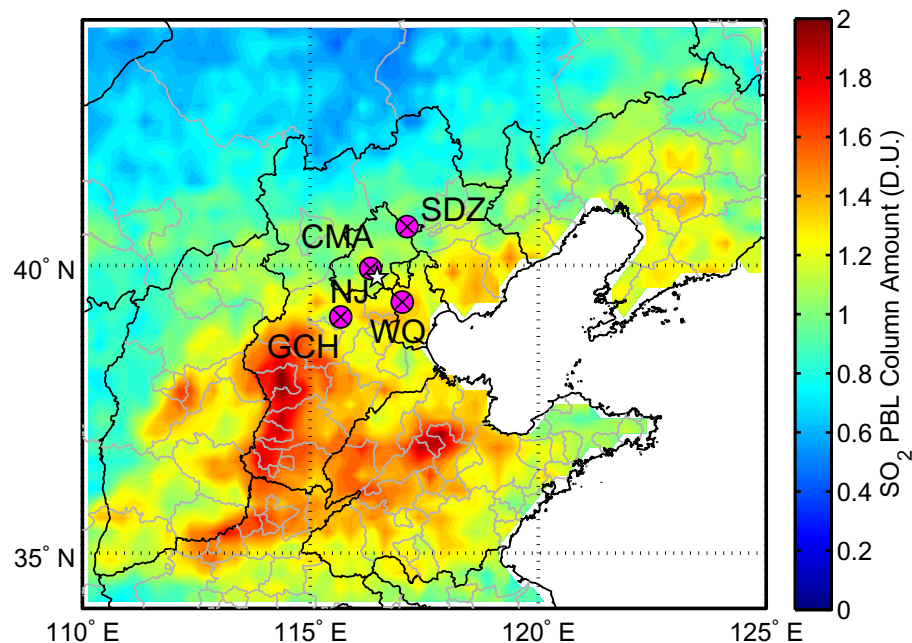


**Fig. 1.** Location of the Shangdianzi (SDZ), China Meteorological Administration (CMA), Gucheng (GCH), Wuqing (WQ) site and the Nanjiao meteorological station (NJ) and the average distribution of OMI SO<sub>2</sub> column concentration in 2009.

[Title Page](#)[Abstract](#)[Introduction](#)[Conclusions](#)[References](#)[Tables](#)[Figures](#)[◀](#)[▶](#)[◀](#)[▶](#)[Back](#)[Close](#)[Full Screen / Esc](#)[Printer-friendly Version](#)[Interactive Discussion](#)

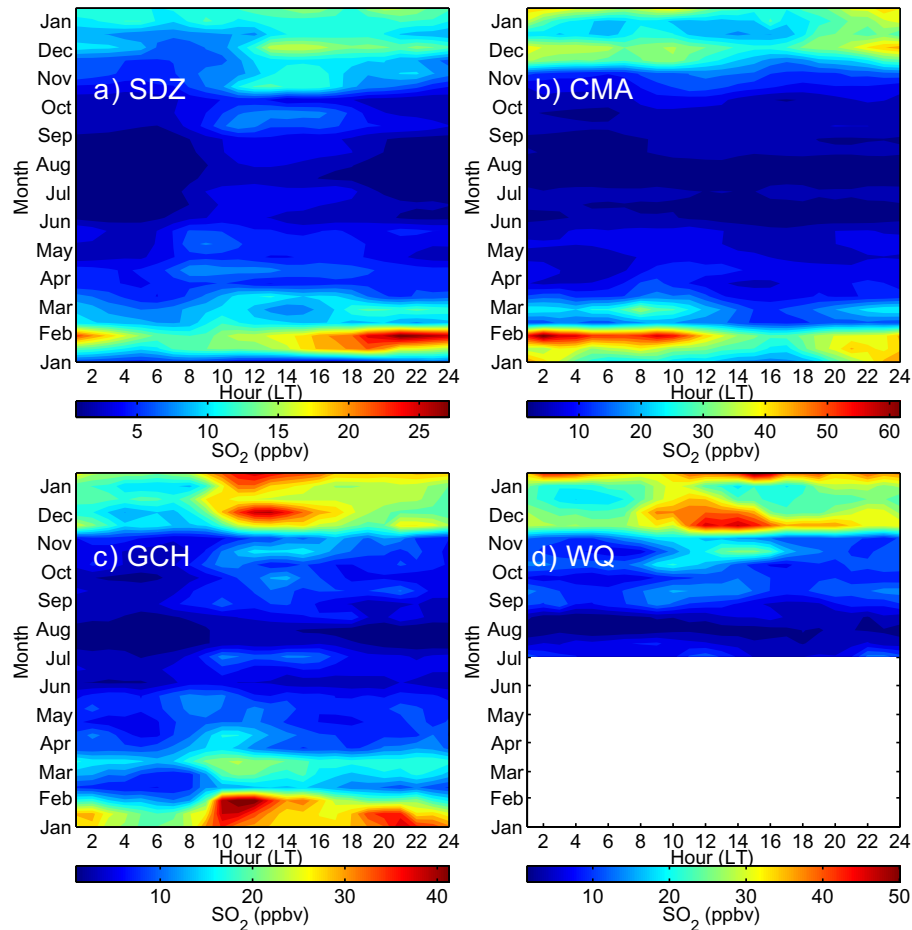


**Fig. 2.** Diurnal and seasonal variation of  $\text{SO}_2$  concentrations at the (a) Shangdianzi, (b) China Meteorological Administration, (c) Gucheng and (d) Wuqing site.

**$\text{SO}_2$  noontime peak phenomenon in the North China Plain**

W. Y. Xu et al.

Title Page

Abstract Introduction

Conclusions References

Tables Figures

◀ ▶

◀ ▶

Back Close

Full Screen / Esc

Printer-friendly Version

Interactive Discussion



## SO<sub>2</sub> noontime peak phenomenon in the North China Plain

W. Y. Xu et al.

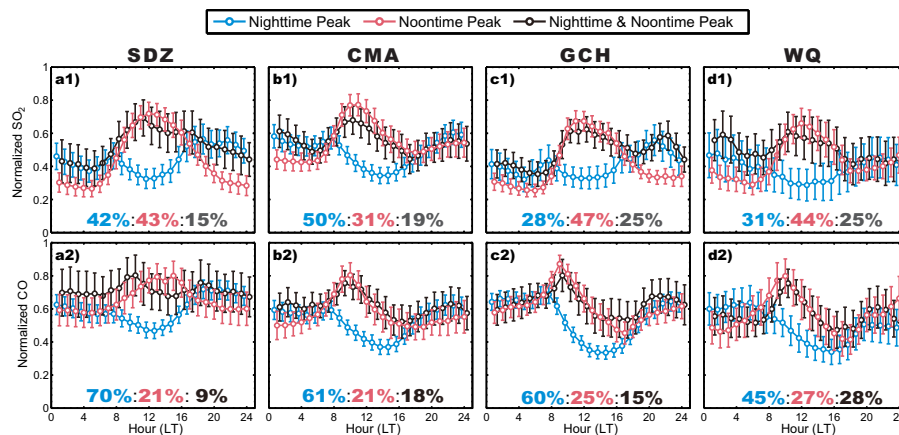


**Fig. 3.** Normalized (1) SO<sub>2</sub> and (2) CO diurnal variation pattern for the days with peaks occurring during nighttime (blue, before 9 a.m. or after 16 p.m.), noontime (red, between 9 a.m. and 16 p.m.) and during both nighttime and noontime (black) at **(a)** Shangdianzi, **(b)** China Meteorological Administration, **(c)** Gucheng and **(d)** Wuqing station. The circle and error bar represent the average value  $\pm 3$  standard error of the mean.

Title Page

Abstract

Introduction

Conclusions

References

Tables

Figures

◀

▶

◀

▶

Back

Close

Full Screen / Esc

Printer-friendly Version

Interactive Discussion



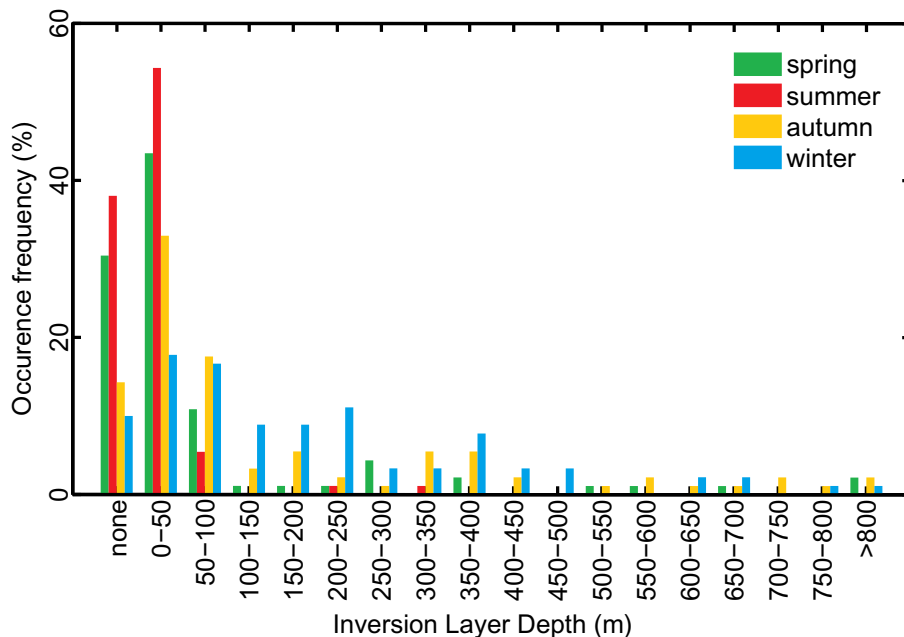


**Fig. 4.** The occurrence frequency of different temperature inversion layer depths during spring (March–May 2009), summer (June–August 2009), autumn (September–November 2009) and winter (December 2009–February 2010) in the 08:00 LT radiosonde data.

**SO<sub>2</sub> noontime peak phenomenon in the North China Plain**

W. Y. Xu et al.

Title Page

Abstract Introduction

Conclusions References

Tables Figures

◀ ▶

◀ ▶

Back Close

Full Screen / Esc

Printer-friendly Version

Interactive Discussion



## SO<sub>2</sub> noontime peak phenomenon in the North China Plain

W. Y. Xu et al.

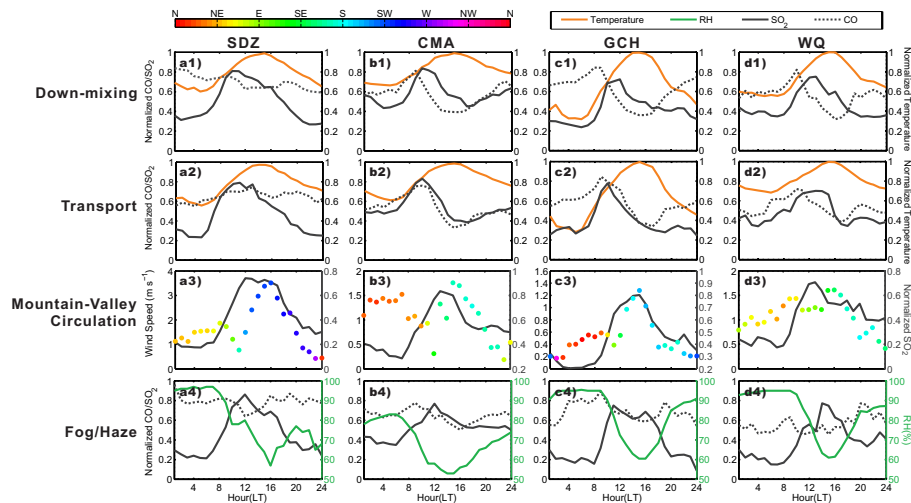


**Fig. 5.** Averaged diurnal variation patterns for (1) the PBL down-mixing, (2) the plume transport, (3) the mountain valley breeze and (4) the fog/haze case for (a) Shangdianzi, (b) China Meteorological Administration, (c) Gucheng and (d) Wuqing.

Title Page

Abstract

Introduction

Conclusions

References

Tables

Figures

◀

▶

◀

▶

Back

Close

Full Screen / Esc

Printer-friendly Version

Interactive Discussion



**SO<sub>2</sub> noontime peak phenomenon in the North China Plain**

W. Y. Xu et al.

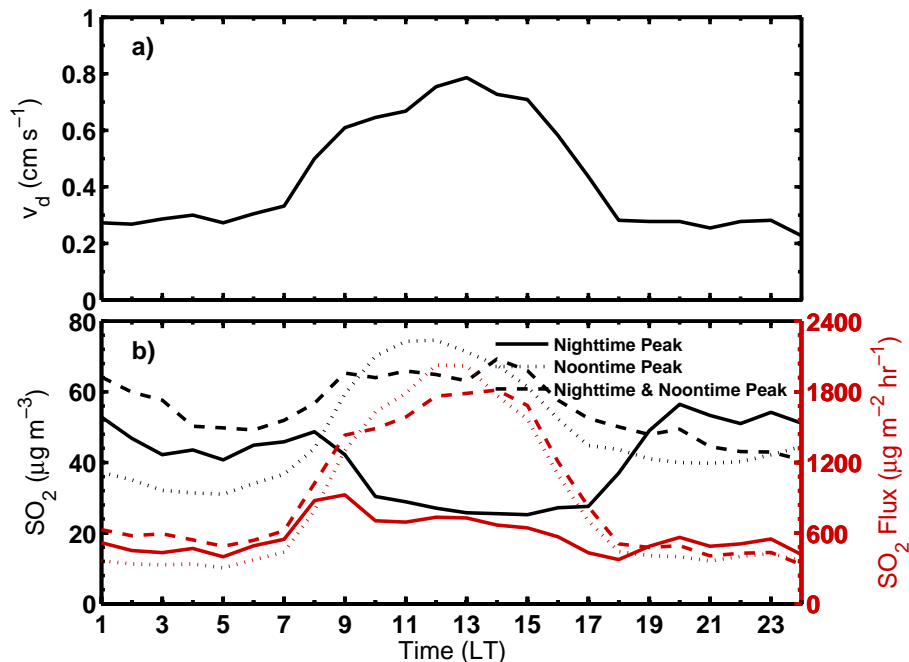


**Fig. 6.** (a) Diurnal variation of the dry deposition velocity inferred from Tsai et al. (2010); (b) Calculated dry deposition fluxes (red lines) based on the three characteristic SO<sub>2</sub> diurnal variation patterns (black lines) in Wuqing during autumn 2009.

SO<sub>2</sub> noontime peak phenomenon in the North China Plain

W. Y. Xu et al.

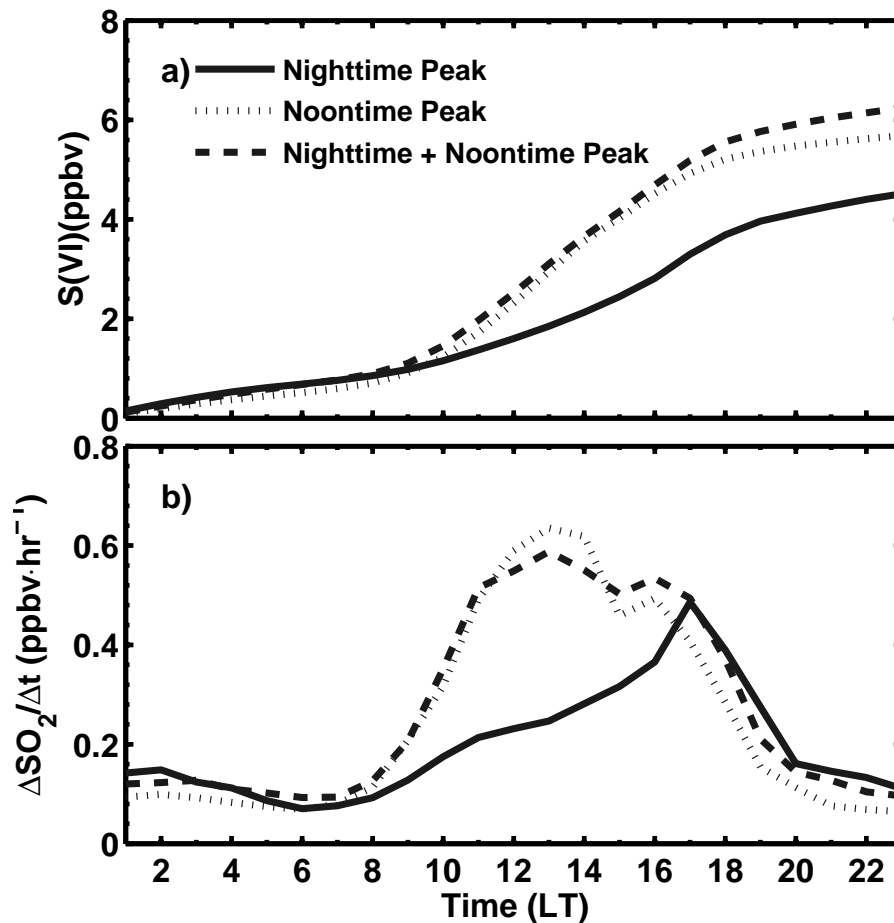
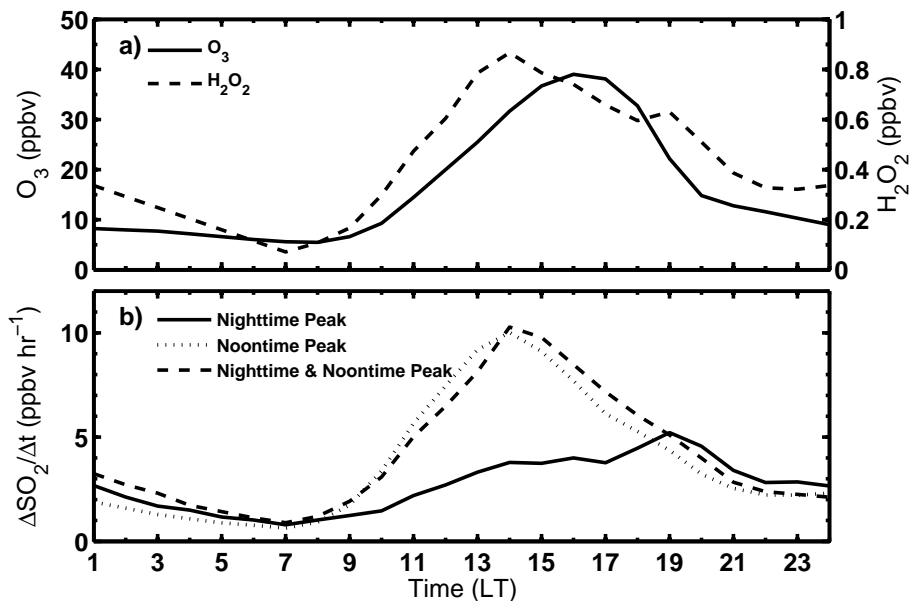


Fig. 7. Simulated gas phase oxidized SO<sub>2</sub> (a) amount and (b) oxidation rates based on the three characteristic SO<sub>2</sub> diurnal variation patterns in Wuqing during autumn 2009.

## SO<sub>2</sub> noontime peak phenomenon in the North China Plain

W. Y. Xu et al.



**Fig. 8.** (a) O<sub>3</sub> and H<sub>2</sub>O<sub>2</sub> diurnal profiles used in the estimations; (b) Estimated aqueous phase oxidized SO<sub>2</sub> amount based on the three characteristic SO<sub>2</sub> diurnal variation patterns in Wuqing during autumn 2009.

[Title Page](#)[Abstract](#)[Introduction](#)[Conclusions](#)[References](#)[Tables](#)[Figures](#)[◀](#)[▶](#)[◀](#)[▶](#)[Back](#)[Close](#)[Full Screen / Esc](#)[Printer-friendly Version](#)[Interactive Discussion](#)